DOI: 10.2478/ijasitels-2025-0009

SDR receiver for power measurement with internal noise compensation

Iulian Bouleanu[1], Mădălina Antoneac[1], Macarie Breazu[1], Alina Cristina Viorel[1], Gabriela Crăciunaș[1]

[1]Computer Science and Electrical and Electronics Engineering Department, Faculty of Engineering, "Lucian Blaga" University of Sibiu, Romania

{iulian.bouleanu, madalinamaria.antoneac, macarie.breazu, alina.viorel, gabriela.craciunas} @ulbsibiu.ro

Abstract

This paper presents a solution for implementing a power measurement receiver made with PlutoSDR. The paper proposes the dynamic elimination of the contribution of internal noise to the measured signal level by compensating with the level of internal noise produced by the receiver in the adjacent RF band. Our approach is based on the fact that the internal noise level in the working band is approximately equal to that in the frequency band in the immediate vicinity. As far as we know, our work is the first to use the idea of measuring the noise in an adjacent band to estimate the internal noise of the measuring instrument. Another aspect necessary to ensure a complete measurement solution that does not require pre-measurement calibration concerns the compensation of the nonlinearities of the reception path. The compensation was automatically performed by modifying the amplification of the reception path depending on the working frequency. For high levels of the measured CW signal (-50 dBm ... -10 dBm) the solution allows obtaining measurement errors of less than 0.55 dB. From the perspective of measurement uncertainty, with a value of $U = \pm 1$ dB (k=2), the instrument with the method used fits very well into the requirements for pre-compliance EMC measurements. For levels lower than -60 dBm, the error starts to increase rapidly, so that at values of -70 dBm the signal can no longer be measured.

Keywords: Software Defined Radio (SDR), Spectrum Analysis, Internal Noise Correction, Signal Processing

1 Introduction

The electromagnetic spectrum represents one of the most valuable resources of the modern interconnected world. In a time when wireless applications have experienced explosive growth, accurate monitoring and measurement of energy levels of electromagnetic waves is absolutely necessary to verify compliance with international regulations on human exposure to EM fields or to ensure the electromagnetic compatibility of electrical and electronic systems [7].

Conventional spectrum analyzers, although more accurate, are much more expensive, heavier and bulkier and are not suitable for continuous electromagnetic field mobile monitoring situations.

The purpose of this article is to present a solution for the design and calibration of an electromagnetic field measurement receiver that is sufficiently accurate, lightweight and cost-effective in order to facilitate measurements under mobile conditions by placing, for example, the entire measurement system on a drone. The key to achieving low costs and low weight is the use of SDR technology.

Software Defined Radio (SDR) is a flexible radio communication architecture where traditional hardware operations realized by analogical components - mixers, filters, amplifiers, modulators - are replaced by software algorithms running on a general-purpose processor or FPGA [14].

In a typical SDR system the analog front-end converts incoming electromagnetic waves into an intermediate frequency (IF) or baseband signal, which is then digitized by an Analog-to-Digital Converter (ADC). The digital signal is processed through a sequence of algorithms which performs operations such as filtering, demodulation, and spectral analysis [13]. This approach is possible as a result of using the equivalent bandgap theorem [16]. The front-end analog converter translates the spectral components contained in the RF band of interest to much smaller frequency values, to which the sampling theorem can be applied, maintaining the shape of the spectral density distribution.

In [3] Costouri et al. use the idea of measuring the noise in the adjacent band to estimate the external noise. As far as we know, our work is the first to use the idea of measuring the noise in an adjacent band to estimate the internal noise of the measuring instrument.

2 Theoretical Background and Method

2.1 Electromagnetic radiation

Electromagnetic (EM) radiation encompasses oscillations of electric and magnetic fields that propagate through space. These oscillations transport energy, and their behavior depends on parameters such as frequency, wavelength, phase and amplitude [9]. The electromagnetic spectrum covers all possible frequencies from near zero Hertz to infinite.

Electromagnetic waves can be produced naturally by a series of phenomena but also artificially with technologies developed by humanity in the last two centuries. As new technologies have begun to use more and more frequency bands, the problem of monitoring the electromagnetic spectrum in order to achieve effective management has become increasingly acute.

Sources generating electromagnetic waves produce spectral components in different widths of frequency bands and can propagate over significant distances. From a human perspective, they can be useful (for example, when they carry information) or parasitic (when they disrupt the functioning of some systems or create radiation dangerous to human health).

Signal propagation is influenced by path loss, atmospheric absorption, diffraction, and multipath reflection [5]. The power density (S) of an electromagnetic wave decreases proportionally to the square of the distance (r) [9], [16]:

© 2025 Lucian Blaga University of Sibiu

$$S = \frac{P_t}{4\pi r^2} \quad (1)$$

where P_t is the transmitted power.

The power density of a source that generates electromagnetic waves is distributed in a continuous spectrum of frequencies and its level can vary both due to the propagation conditions and due to the operating principle of the source. As a result of the superposition of contributions from two or more sources, at each point in space there are different power distributions for the entire frequency spectrum.

Any electronic equipment, including those designed to perform measurements, generates parasitic electromagnetic waves by their very operation. These waves contribute to the formation of an electromagnetic noise floor that establishes the minimum threshold of an external electromagnetic wave that can be measured.

A signal in the frequency domain is typically represented by its Power Spectral Density (PSD), which quantifies power per unit bandwidth [11]:

$$PSD(f) = \frac{|X(f)|^2}{B} \quad (2)$$

where $X(f)$ is the Fourier transform of the time-domain signal $x(t)$ and B is the observation bandwidth.

The accurate estimation of PSD is central to EM field measurements. Modern communication networks operate across shared frequency bands [7]. To prevent interference and ensure compliance with emission regulations, continuous spectrum monitoring is necessary [7].

2.2 Mathematical model of real-time spectrum measurement

In order to correctly evaluate the EM field level at the receiver input it is necessary to mathematically model the contribution of internal noise and amplification variations produced by the translation of the spectrum from RF to the equivalent baseband at the signal processing stages.

Signal power can be evaluated in both the time domain and the frequency domain. In the frequency domain the evaluation involves summing the power contribution of each spectral component in the RF band. In the time domain the power is obtained by calculating an average value of the power of the measured signal samples over a large number of periods.

Since evaluating power in the time domain requires less processing power (it does not also require performing FFT), this solution was chosen in this work.

Let x(t) represent th e received signal at the SDR input. The measured digital signal *y(t)* after amplification and filtering can be expressed as [15]:

$$y(t) = G(t) \cdot x(t) + n(t) \quad (3)$$

where *G(t)* is the time-varying system gain, and *n(t)* represents additive noise (thermal + quantization).

The instantaneous power $P_{inst}(t)$ is computed as:

© 2025 Lucian Blaga University of Sibiu

$$P_{inst}(t) = |y(t)|^2 \quad (4)$$

The mean received power over a time window *T* is [17]:

$$P_{avg} = \frac{1}{T}\int_0^T |y(t)|^2 dt \quad (5)$$

Expressed in logarithmic form, the result is [12]:

$$P_{dBm} = 10 \cdot \log_{10}\left(\frac{P_{avg}}{1mW}\right) \quad (6)$$

To compensate for internal offsets, noise and nonlinearity, a correction factor (C_{corr}) is introduced [18]:

$$P_{corr} = P_{dBm} - C_{corr} \quad (7)$$

Into the correction factor, two components can be identified:

$$C_{corr} = C_{nonlin} + C_{noise} \quad (8)$$

where:

- C_{nonlin} will correct the amplification nonlinearities of the radio reception down-convertor path branch in PlutoSDR.
  This can be determined as the difference between the actual, correct level of a CW signal and the level displayed by the receiver:

$$C_{nonlin} = P_{real_{dBm}} - P_{meas_{dBm}} \quad (9)$$

- C_{noise} will correct for internal noise produced by the receiver operation. Internal noise is a major limitation in SDR-based measurements [10]. Mixer leakage, quantization artifacts and the intermodulation products due to the nonlinear operation of some reception path stages introduce unwanted energy that affects power readings. The proposed system compensates for these effects by measuring the baseline noise floor when external signal is present C_{int_noise} correction constant is derived as:

$$C_{noise} = 10 \cdot \log_{10}\left(\frac{P_{noise}}{1mW}\right) \quad (10)$$

  where P_{noise} is the measured internal noise power in the immediate vicinity of the measured signal. In this category, in addition to thermal noise and quantization noise, leakage due to the local oscillator (LO) as well as parasitic products resulting from the nonlinear operation of some stages on the reception path will also have to be taken into account. Except for LO leakage, the other internal noise components are additive and dependent on the real-time bandwidth.

Thermal noise depends on the bandwidth of the signal taken into real-time analysis and can be determined mathematically with:

$$P_{th\_noise_{dB}} = 10 \cdot \log_{10}(kTB) \quad (11)$$

where: k – Boltzmann constant (1,38·10−23), T - receiver operating temperature in degrees Kelvin and B - real-time bandwidth.

To evaluate the power according to (5) a moving average filter of *N* samples is used to smooth measurement fluctuations:

© 2025 Lucian Blaga University of Sibiu

$$P_{filtered}[k] = \frac{1}{N}\sum_{i=0}^{N-1} P_{corr}[k-i] \quad (12)$$

This process stabilizes output readings and eliminates short-term variations.

2.3 Calibration Method

The calibration method involves dynamically changing the value of the correction coefficients C_{nonlin} and C_{noise} in the signal processing flow. These correction terms need to be subtracted from measured power levels.

The nonlinearity coefficient of the reception path, C_{nonlin}, is specific to each receiver and can be obtained with the measurement setup shown in Fig. 1.

A calibrated signal generator provides a controlled RF signal, which is transmitted to the SDR platform acting as the receiving and processing device. In order for the level value at the signal generator input to be within a known error margin, a characterized RF cable must be used. The SDR platform captures the input signal and forwards it to a computing system running the GNU Radio software environment, where the digital signal processing flow is implemented. Within GNU Radio, several processing blocks perform filtering, power estimation, and visualization of the measured spectrum in real time.

The value of nonlinearity coefficient is frequency dependent and its determination requires measurements across the entire SDR platform frequency band on as many frequencies as possible. For each frequency into a chosen frequency set the actual level at the SDR input is compared with the level displayed after processing by the GNU Radio power measurement application.

The noise coefficient, C_{noise}, is also specific to each receiver. It is a well-known problem with SDR receivers that they produce parasitic components near zero frequency that form a peak. This is due to the coupling of the mixer with the local oscillator, the imperfections of the mixer, the offset of the amplifiers and the differences between the I and Q branches. For a more accurate assessment of the received signal level, it is desirable to avoid translating the measured signal spectrum over this spike.

In this situation, if the spectrum of the measured signal can be placed completely on one side or the other of the zero frequency, the other half can be used as a reference for evaluating the C_{noise}. The fact from which this work starts is that in this band, if it does not contain other external signals, the level of internal noise is approximately the same value as that in the measured signal band.

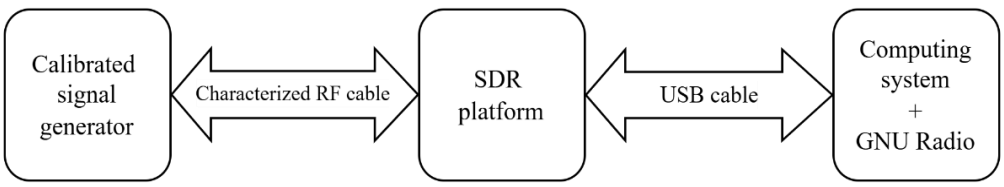

Figure 1. Block diagram of the measurement system used to determine the nonlinearity coefficient

© 2025 Lucian Blaga University of Sibiu

3 Implementation, measurements and results

3.1 ADALM PlutoSDR

Pluto SDR is a SDR platform made by Analog Devices. This platform can digitize, process, and analyze radio signals in software, allowing flexible and reconfigurable implementations without specialized analog components [14].

PlutoSDR operates natively within the frequency range of 325 MHz to 3.8 GHz, a limitation determined by its internal components, particularly the AD9363 Radio Frequency Integrated Circuit (RFIC), which is optimized for this range. However, the device can be customized to extend its operational bandwidth, covering frequencies from 70 MHz up to 6 GHz [1]. This customization is achieved through a software modification involving a firmware update, which enables additional capabilities of the AD9363 RFIC that are normally disabled by default [1].

The device provides 12-bit ADC resolution and communicates via USB2.0 with a laptop or a desktop where data will be processed with GNU Radio, MATLAB or other SDR frameworks.

GNU Radio provides a graphical flow-based interface (GNU Radio Companion, GRC) that allows the design of signal processing chains without need of complex programming [4].

3.2 Flowchart for power measurement

The signal received by PlutoSDR via cable from the signal generator is first down-converted in frequency around the value of zero, digitized by the ADC located in PlutoSDR and passed into the computing system through the USB2.0 socket where GNU Radio perform data processing. The sequence of processing blocks used is presented in Figure 2.

The data is fed into the processing flow by the PlutoSDR Source block. It controls the reception side of the PlutoSDR platform by setting, among other things, the reception frequency (LO Frequency), the RF bandwidth and the receiver gain. The gain must be set manually so that it does not automatically adapt to the measurement conditions by introducing an uncontrollable variable into the received signal amplification chain. The sampling frequency is set with the *samp_rate* variable to the value of 196kHz.

The data from the PlutoSDR Source output are complex numbers that represent the I and Q values of the equivalent baseband signal samples. Because the RF signal is brought directly into the equivalent baseband and not on an intermediate frequency, if we view the signal spectrum at this point, we will notice parasitic components due to the frequency shift process performed on the PlutoSDR receive path.

© 2025 Lucian Blaga University of Sibiu

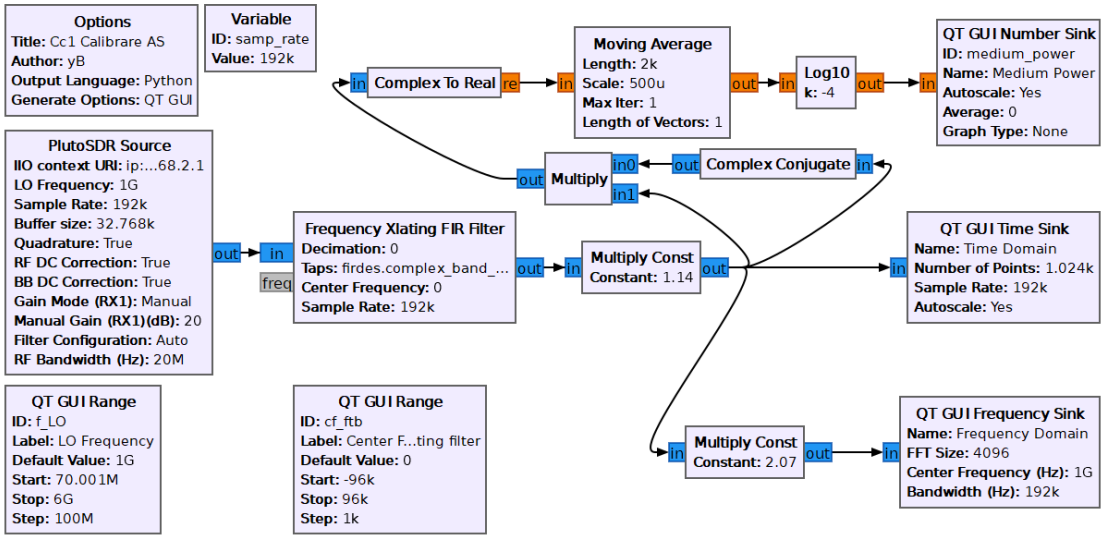

Figure 2. GNU Radio flowgraph of the SDR-based measurement chain

In order for the parasitic near zero components not to affect the measured signal, it is desirable that the spectrum of interest does not overlap the zero frequency. This is achieved with the Frequency Xlating FIR Filter, which can move the spectrum of interest around the zero frequency with a maximum value of (+/-)*samp_rate*/2. The center frequency of the XLating filter will be changed with the slider made with QT GUI Range with id: *ct_ftb*. Being a filter, it will also allow interactive filtering of spectral components [6]. Changing the bandwidth of this filter will introduce changes in the correction coefficients, but the analysis of these changes is not the subject of this study.

The Multiply Const blocks used in the processing flow will increase / decrease the value of the samples. They are used to allow the final level to be adjusted regardless of the working frequency and bandwidth. In order to achieve visual feedback regarding the level and shape of the measured signal, we considered it is necessary to present the result in three display modes:

1. In the time domain, with QT GUI Time Sink.
2. In the frequency domain, with QT GUI Time Frequency Sink.
3. Numerically, by displaying the signal power level, in dBm units, with QT GUI Number Sink.

The power level of the received signal is computed in the following steps:

1. The instantaneous power of each sample is obtained, according to (4), by multiplying the value by the complex conjugate of the value, and subsequently transforming the result into a real number (Complex to Conjugate, Multiply, Complex to Real).

2. Calculate the average power over a large number of periods N, according to (5), respectively (11) with the Moving Average block. The power is in linear power units.

3. Obtain the value in dBm according to (6) with the Log10 block.

© 2025 Lucian Blaga University of Sibiu

3.3 Calibration

To obtain reliable results, the characterization of the device was performed using a calibrated signal generator Anna Pico APSIN20G [2].

A frequency step of 100 MHz is established and the PlutoSDR working band is divided by this value, determining the frequencies at which the frequency coefficients will be determined. Therefore, all measurements in this study will be performed on the same set of frequencies uniformly distributed in the range of 70 MHz to 6 GHz.

In a first step, the values of the multiplication constants in the processing flow will have to be set up. With the signal generator, a continuous wave (CW) signal with a level of -50 dBm is generated and the entire frequency band is scanned to identify the frequency at which the level is maximum. The constants are modified so that the displayed level is -50 dBm. It is taken into account that the cable between the generator and PlutoSDR has an attenuation that increases with frequency.

In the case of the PlutoSDR used, f_{LO}=4 GHz, C_1=1.14, C_2 = 2.07 and k= -4 were identified. The measurement result can be seen in the graphical user interface shown in Fig. 3. The measured signal is of the CW type: a single spectral component of -50dBm level in the frequency domain and two sinusoidal components, affected by noise, in the time domain (representing the real and imaginary part).

This is the signal that we want to measure with the highest possible accuracy. The noise floor is at -110 dBm. The spectral component corresponding to the 4 GHz frequency is shifted by approximately 50 kHz and is due to the PlutoSDR LO generator (adjusting this deviation is not the subject of this study). On the left side of this component (where PlutoSDR shows 4 GHz) a group of spectral components in a bandwidth of a few kHz is observed. These frequencies represent the near-zero parasitic spike components. In the spectral domain, a group of other parasitic components is also observed, with values

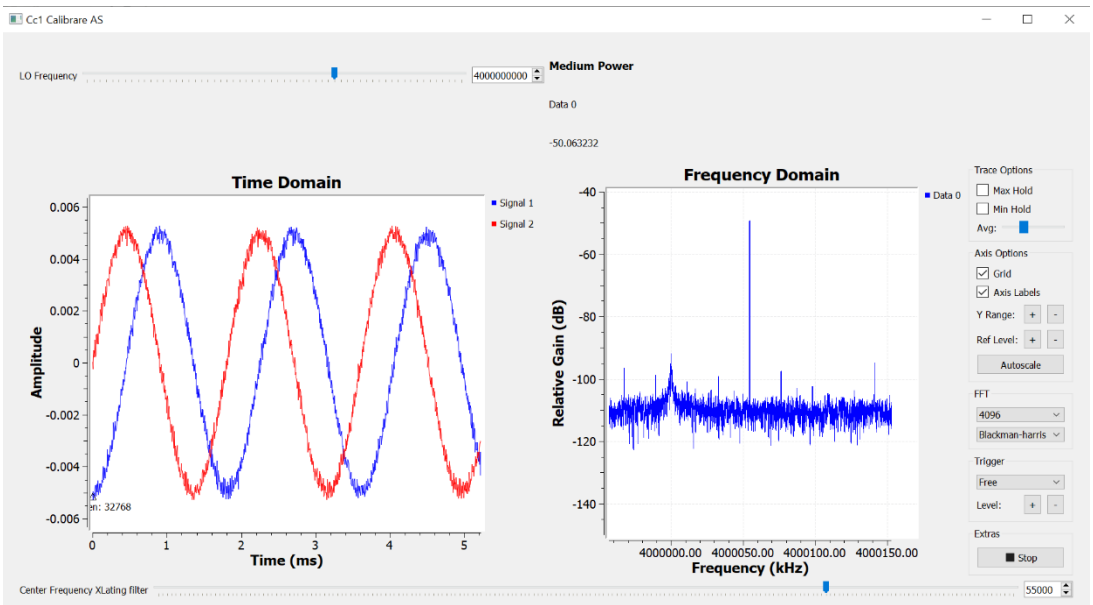

Figure 3. GUI with results for f_{LO}=4 GHz and N=-50dBm

© 2025 Lucian Blaga University of Sibiu

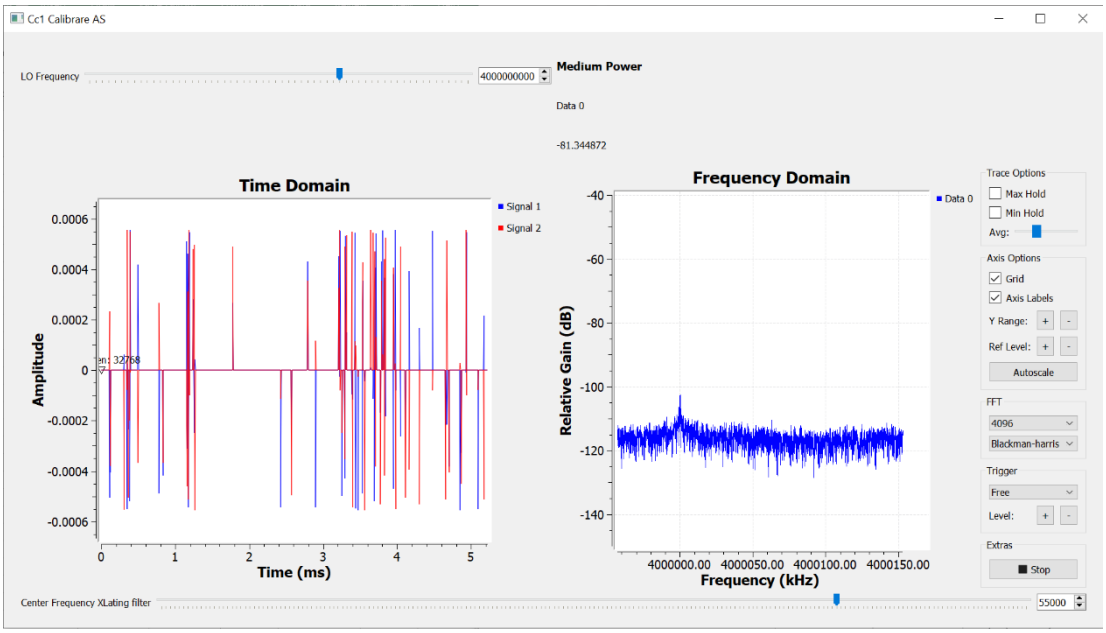

Figure 4. GUI with results for no signal (only internal noise)

of approximately 10 dB above the noise floor. These, together with the near-zero spike components but also with a large part of the noise floor value, must be compensated using the coefficient C_{noise}. If these components due to internal noise did not exist, the noise floor should be made only by the thermal noise components.

The results in Fig. 4 are obtained in the absence of an RF signal with the measurement system in Figure 1. The RF cable was disconnected and a 50 Ohms load was connected to the Pluto SDR receiving antenna.

For the bandwidth used in this application (192kHz), according to (11) the thermal noise contribution is -121 dBm. Comparing the results in Fig. 3 with those in Fig. 4 we find that a difference of approximately 40 dB is due to the other types of noise except thermal. Upon closer analysis we find that in Fig. 3, outside the spectral component of the measured signal positioned at approximately 4 GHz, a series of other spectral components appear visible arranged above the noise floor with levels of approximately 10 dB.

These, together with those that in Fig. 3 versus Fig. 4 raise the noise floor by a level of approximately 10 dB, are parasitic signals caused by the processing of the measurement signal on the reception path. They are easy to visualize because we know that the measured signal must contain only one spectral component because it is CW. If the bandwidth of the measured signal were larger, these could no longer be separated.

We conclude that, where it possible to estimate C_{noise} in the presence of signal, this could lead to an increase in the accuracy of the measurement.

© 2025 Lucian Blaga University of Sibiu

3.4 Power measurements with internal noise compensation

In order to perform this operation dynamically without the need to modify the hardware setup before each measurement, we propose that the noise level estimation be performed in the immediate vicinity of the measured signal band, on the same bandwidth. The solution we have used in this study is: divide the received bandwidth into two equal parts with respect to the zero value, translate the entire spectrum of the measured signal into one of the two halves, measure the signal power on each of these and extract the noise power from the measured signal which contains both the useful signal and the noise.

If, after frequency tuning, the spectrum of the signal to be measured is at positive frequencies, the two Frequency Xlating filters will separate the input data so that the positive part of the spectrum (signal + noise) will be processed on the upper branch and the negative part of the spectrum (noise) on the lower branch.

If no signal is applied at the input, the difference between the power of the samples processed on the two paths is -380 dBm, so the two lines are balanced. When introducing a useful signal with a frequency of 4 GHz from the signal generator, for a dynamic range between -60 dBm and -10 dBm the average error is below 1 dB. At the other frequencies in the PlutoSDR working range the average error increases to differences of +/- 4,15 dB, an aspect due to the non-uniformity of the receiver's amplification.

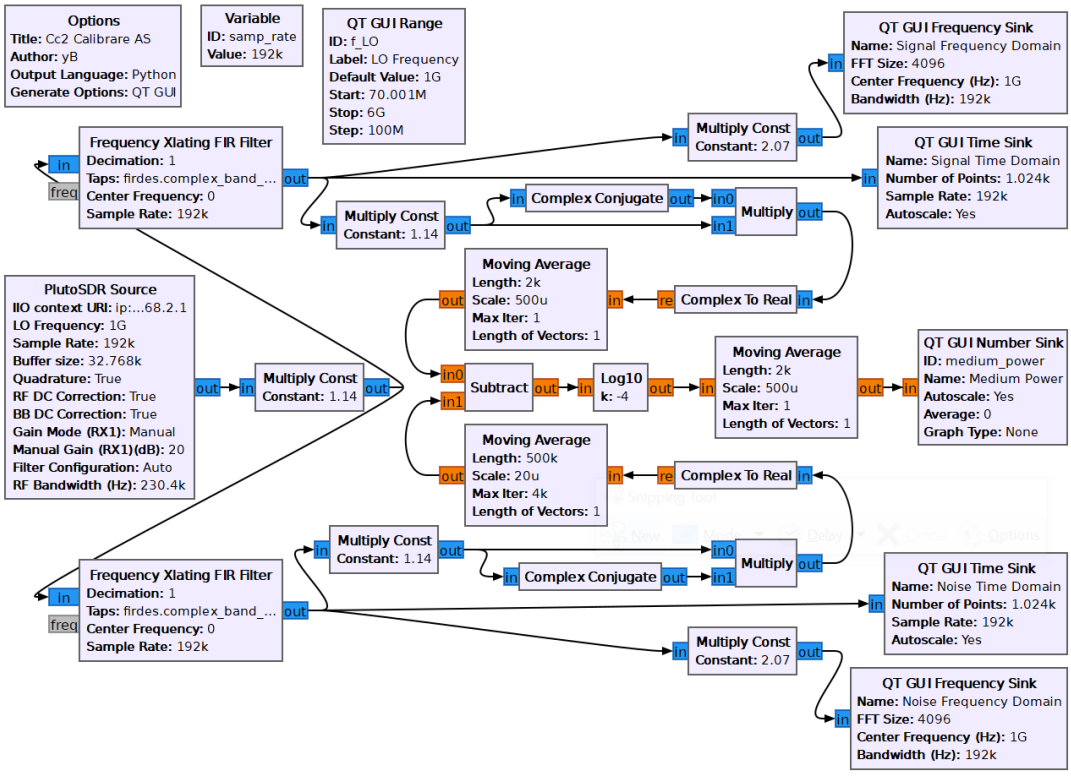

Figure 5. Flowchart for power measurements with internal noise self-compensation

© 2025 Lucian Blaga University of Sibiu

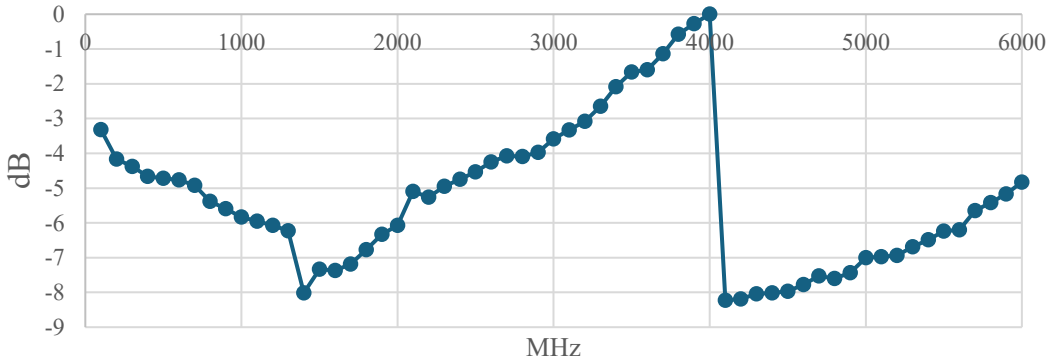

Figure 6. PlutoSDR radio receiver amplification characteristic (C_{nonlin})

To determine the nonlinearity compensation coefficient, C_{nonlin}, an experiment was performed using the measurement scheme in Fig. 5 and the following algorithm:

1. For each frequency, the previously determined measurement coefficient is taken into account.
2. For each frequency, a CW signal with $N_{generator} = N_{inSDR} + a_{cable}(f)$ is generated from a calibrated signal generator (AnaPico APSIN20G), where $a_{cable}(f)$ is the amount of attenuation introduced by the RF cable between the generator and PlutoSDR and $N_{inSDR} = -50dBm$
3. The level is measured with the Fig. 5 flowchart.
4. The value of the correction factor is computed as the difference between the real level and the measured level.

The results are presented in Fig. 6. The nonlinearity coefficient is added to the value of the Gain parameter in the PlutoSDR Source block so that the receiver compensates the gain depending on the working frequency.

3.5 Results

After modifying the flowchart so that the correction is performed dynamically, measurements were performed on all frequencies in the set with input signal values in the range - 60dBm ...- 10 dBm. A summary of these results is presented in Table 1.

Table 1. An excerpt of measurement results

N_{inSDR} [dBm]	N_{meas} [dBm]							$\lvert\Delta N_{max}\rvert$ [dB]
	0.1 GHz	**1 GHz**	**2 GHz**	**3 GHz**	**4 GHz**	**5 GHz**	**6 GHz**	
-10	-10.41	-10.55	-10.40	-10.28	-10.30	-10.02	-10.00	0.55
-20	-20.05	-20.19	-20.06	-19.98	-20.20	-20.13	-20.17	0.20
-30	-30.12	-30.34	-30.11	-29.75	-30.20	-30.24	-30.13	0.34
-40	-40.00	-40.09	-39.90	-39.60	-40.00	-39.88	-40.02	0.40
-50	-49.98	-50.02	-49.97	-49.50	-50.00	-49.99	-50.02	0.50
-60	-61.16	-61.30	-61.08	-60.51	61.16	-60.99	-61.26	1.30

© 2025 Lucian Blaga University of Sibiu

3.6 Measurement uncertainty

The receiver power level (dBm) measurement uncertainty was evaluated based on an uncertainty budget that includes the contributions of the APSIN20G generator, the Withwave W701-SM1SM1-1m measurement cable and the receiver to generator calibration residual.

The measurements were performed in the range 100 MHz – 6 GHz, with a step of 100 MHz, for input levels appropriate to the receiver's range of use. At each frequency point the difference was determined (Table 1):

$$\Delta N = N_{inSDR} - N_{meas} \tag{13}$$

The observed experimental differences were |ΔP| < 0.55 dB over the entire frequency range.

When assessing the uncertainty, the following were taken into account:

- Declared uncertainty of the APSIN20G generator [2] in the 0.2–5.5 GHz band, $U_{APSIN} = \pm 0.6$ dB, for which the standard uncertainty $u_{APSIN} \approx 0.35$dB is obtained.
- An overall tolerance of +/-0.2 dB for the Withwave W701-SM1SM1-1m cable, for which the standard uncertainty $u_{cable} \approx 0.12$dB is obtained.
- Experimentally measured comparison residue, $U_{residue} = \pm 0.55$ dB, for which the standard uncertainty $u_{residue} \approx 0.32$dB is obtained.

Each contribution was treated as a rectangular distribution and the associated standard uncertainties were combined using the root-sum-of-squares (RSS) method.

The resulting combined standard uncertainty is $u_c \approx 0.49\, dB$ which leads to an expanded uncertainty:

$$U = \pm 1 \text{ dB (k=2)} \tag{12}$$

valid for the power level measured in dBm, in the frequency range 100 MHz – 6 GHz, under similar conditions of use and calibration.

3.7 Discussions

When measuring CW signals with levels in the range -50dBm...-10dBm, the measurement scheme responds very well, the maximum error being 0.55 dB. For lower levels the error increases to 1.3 dB for measured signal levels of -60 dB. For levels lower than -60 dB the error increases significantly so that at -70dB, the signal can no longer be measured.

From the visual analysis of the measured signal's spectra with the flow chart in Fig. 5 we found that at some frequencies of the measurement signal and at values higher than -40 dBm intermodulation products appear. Their number and value increase with the signal level. However, the measurement scheme manages to compensate for their contribution to the final result because these intermodulation products are also found in the lower spectrum. If at high levels the scheme performs surprisingly well, at levels lower than -60dBm the results are very poor, practically failing to measure signals with values lower than -65dBm.

© 2025 Lucian Blaga University of Sibiu

With a level uncertainty of ±1 dB the instrument complies:

- with the typical range for EMC pre-compliance systems (±1…3 dB);
- with the lower (better) uncertainty range of commercial pre-compliance receivers (±1.5…2.5 dB);
- below the limits required by CISPR 16 for compliance laboratory equipment (±2 dB).

4 Conclusion

This paper presents a solution for implementing an electromagnetic field strength measurement receiver made with the PlutoSDR platform produced by Analog Device. In order to eliminate the contribution of internal noise to the measured signal value, a dynamic self-calibration solution was used. The solution compensates for the value of the internal noise level produced by the receiver. The principle used is that the level of internal noise in a frequency band in the immediate vicinity of the working band is approximately equal to that in the working band. As far as we know, our work is the first to use the idea of measuring the noise in an adjacent band to estimate the internal noise of the measuring instrument.

A second aspect addressed in the paper (in order to offer a complete measurement solution that does not require pre-measurement calibration) concerns with the compensation of the nonlinearities of the reception path. The compensation was automatically performed by modifying the amplification of the reception path in PlutoSDR depending on the working frequency in order to obtain a flat characteristic of the reception path throughout the working band.

For high levels of the measured CW signal (-10 dBm ... -50 dBm) this solution allows to obtain measurement errors smaller than 0.55 dB. Regarding measurement uncertainty, having a value of $U = \pm 1$ dB (k=2), the instrument (with the method used) fits very well into the requirements for pre-compliance EMC measurements. For levels lower than -60 dBm the error starts to increase rapidly, so the instrument can no longer be used. We assume that the lower limit of the measurement threshold is due to the low amplification used in the amplification chain (20 dB). This hypothesis will be the subject of a new study in which the quality of the solution will be verified also in the case of broadband signal measurements.

References

[1] Analog Devices, *ADALM-Pluto SDR Active Learning Module, Technical Documen*tation, 2023.
[2] AnaPico *APSIN20G Datasheet*, https://www.testequipmenthq.com/datasheets/ANAPICO-APSIN20G-Datasheet.pdf, accessed 03.11.2025
[3] Costouri, J. Nessel and G. Goussetis, "Validation of a Digital Noise Power Integration Technique for Radiometric Clear Sky Attenuation Estimation at Q-Band," in IEEE Transactions on Antennas and Propagation, vol. 68, no. 9, pp. 6743-6751, Sept. 2020, doi: 10.1109/TAP.2020.3001452.
[4] E. Blossom, *GNU Radio: Tools for Exploring the Radio Frequency Spectrum*, Linux Journal, 2004.
[5] Goldsmith, A., *Wireless Communications*, Cambridge University Press, 2005.
[6] H. Zhang et al., *Noise Reduction in SDR Measurement Systems Using Adaptive Filters*, IEEE Sensors Journal, 2023.

© 2025 Lucian Blaga University of Sibiu

[7] IEEE, *Standard for Spectrum Management and Measurement*, IEEE Std. 1900.5-2019.
[8] ITU-R, *Radio Regulations - Frequency Allocations*, International Telecommunication Union, 2023.
[9] J. D. Kraus, *Electromagnetics*, McGraw-Hill, 2002.
[10] J. P. Darnell, *Noise Compensation Techniques in Software-Defined Radios*, IEEE Trans. on Instrumentation and Measurement, 2019.
[11] L. Peng, *Spectral Power Estimation Techniques for SDR Systems*, IEEE Trans. on Signal Processing, 2021.
[12] M. Rice, *Digital Communications: A Discrete-Time Approach*, Pearson, 2008.
[13] P. Kenington, *RF and Baseband Techniques for Software Defined Radio*, Artech House, 2005.
[14] R. Mitola, *The Software Radio Architecture*, IEEE Communications Magazine, vol. 33, no. 5, 1995.
[15] S. Haykin, *Communication Systems*, 5th ed., Wiley, 2009.
[16] T. S. Rappaport, *Wireless Communications: Principles and Practice*, Prentice Hall, 2010.
[17] V. Oppenheim and R. W. Schafer, *Discrete-Time Signal Processing*, 3rd ed., Prentice Hall, 2010.
[18] W. B. Cook, *Low-Cost SDR Solutions for EMF Measurement*, Sensors Journal, 2021.

© 2025 Lucian Blaga University of Sibiu